

Photon scattering in the giant resonance region of ^{24}Mg , ^{28}Si , and ^{32}S

R. Alarcon, A. M. Nathan, S. F. LeBrun, and S. D. Hoblit

*Nuclear Physics Laboratory and Department of Physics, University of Illinois at Urbana-Champaign,
Champaign, Illinois 61820*

(Received 26 September 1988)

Cross sections for the elastic and inelastic scattering of monochromatic photons from ^{24}Mg , ^{28}Si , and ^{32}S have been measured for incident photon energies between 17 and 28 MeV, spanning the region of the giant dipole resonance. The cross sections are interpreted in terms of the coupling between the giant dipole resonances built on the ground and 2_1^+ states. A good quantitative description of the energy-averaged cross sections is obtained in the context of the dynamic collective model, provided ^{32}S is a vibrational nucleus and ^{24}Mg and ^{28}Si are prolate and oblate nuclei, respectively. The cross sections for ^{28}Si show considerable structure that is correlated in the elastic and 2_1^+ channels and that is not predicted by the dynamic collective model. The elastic cross section is used to infer the total photoabsorption cross section, which is shown to be somewhat more structured than implied by previous direct measurements.

I. INTRODUCTION

This paper presents a study of the giant dipole resonance (GDR) in the *sd*-shell nuclei ^{24}Mg , ^{28}Si , and ^{32}S using the elastic and inelastic scattering of monochromatic photons. The GDR of these nuclei has been widely studied both experimentally and theoretically, and a recent review by Eramzhyan *et al.*¹ summarizes the current status of our knowledge. The experimental evidence provided by photoabsorption and photodisintegration data indicates that the structure and width of the GDR for *sd*-shell nuclei are complicated problems depending on the energy spread of dipole transitions from a single shell, configurational splitting, and splitting due to deformations of the ground-state nucleus. Theoretical calculations have evolved from Tamm-Dancoff calculations with² and without³ collective correlations, to Hartree-Fock self-consistent-field calculations,⁴ to open-shell random-phase approximation (RPA) calculations.⁵ In general all these calculations have yielded poor agreement with the experimental data, especially regarding the substructure within the GDR.

The primary motivation for the present work is to investigate the question of the degree to which the properties of the GDR in *sd*-shell nuclei are affected by the coupling between the GDR and surface degrees of freedom, such as static deformations and vibrations. There is considerable interest these days in the relation between the structure of the GDR and the shape of the nuclear surface.⁶ High-energy photons emitted during heavy-ion collisions have been interpreted as being due to the statistical decay of the GDR built on highly excited states. The energy spectra of these photons are used to infer the shape of the nuclear surface (e.g., the equilibrium deformation) at high temperature and/or at high angular momentum. In medium and heavy nuclei, the coupling of the GDR to shape degrees of freedom often dominates the structure of the GDR.⁷⁻⁹ It is an open question as to

the degree to which this coupling is important in light nuclei. The present work addresses this question via the elastic and inelastic scattering of photons. In effect, one can directly measure the coupling between the GDR's built on the ground and excited states by measuring and analyzing the cross sections for the inelastic scattering into these states. We will do this for the first excited state in the nuclei studied and interpret the data in the context of the so-called dynamic collective model (DCM).¹⁰ This model provides a direct connection between the measured cross sections and the coupling between the GDR and surface degrees of freedom.

A secondary motivation for this research was the investigation of the overall consistency between the photon elastic scattering cross sections and the photoabsorption cross section. These are intimately related via the optical theorem and a dispersion relation,¹¹ so that one can use the elastic cross sections to test the overall consistency of the photoabsorption cross section and to provide severe constraints on it.¹² We will do this for the specific case of ^{28}Si . Furthermore, we will show that the elastic scattering cross section is extremely sensitive to substructure in the GDR and is an excellent way to test for the presence of unresolved fine structure.

This paper is organized as follows. The experimental technique is described in Sec. II. The interpretation of the data is presented in Sec. III, where we use the DCM and the shell model to interpret the elastic and inelastic cross sections. In addition we use both the photoabsorption and (*p*, γ_0) measurements to infer cross sections for elastic photon scattering from ^{28}Si and compare them with the present measurements. Our conclusions are summarized in Sec. IV.

II. EXPERIMENTAL TECHNIQUE

Cross sections for the elastic and inelastic scattering of photons were measured for targets of ^{24}Mg , ^{28}Si , and ^{32}S

between approximately 17 and 28 MeV. These measurements utilized incident beams of quasimonochromatic photons from the University of Illinois tagged-photon facility and a large-crystal NaI spectrometer to detect the photons scattered at an angle of 135° . The average energy resolution of the photon beam was about 160 keV. Metallic targets of ^{nat}Mg (79% ^{24}Mg) and ^{nat}Si (92% ^{28}Si) were used with areal densities of 4.47 and 7.03 g/cm², respectively. For sulfur a powder target of ^{nat}S (95% ^{32}S) was used with an areal density of 5.45 g/cm². The first excited state for the nuclei ^{24}Mg , ^{28}Si , and ^{32}S is a 2^+ state with an excitation energy of 1.37, 1.78, and 2.23 MeV, respectively.¹³ Since the combined energy resolution of the NaI spectrometer and the incident photon beam was between 500 and 800 keV for the energy range under consideration, a complete separation between the elastic and the inelastic scattering to the 2_1^+ level was easily achieved in all cases. Typical spectra are shown in Fig. 1 together with the peak shapes used in the fitting procedure. These peak shapes were determined in a supplemental calibration experiment in which the NaI spectrometer was placed directly into the tagged-photon beam. A more complete description of this experimental technique and the method used to extract absolute cross sections from the data has been presented elsewhere.^{8,12} These cross sections are presented in Figs. 2–4, which we now discuss.

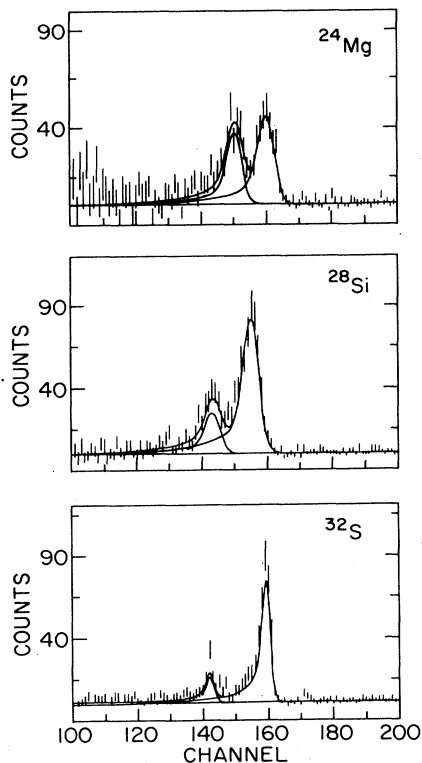


FIG. 1. Measured spectra of scattered photons from ^{24}Mg , ^{28}Si , and ^{32}S at 21.5 MeV incident energy. The curves are the results of a two-peak fit to the data in order to separate the scattering into elastic and 2_1^+ inelastic components.

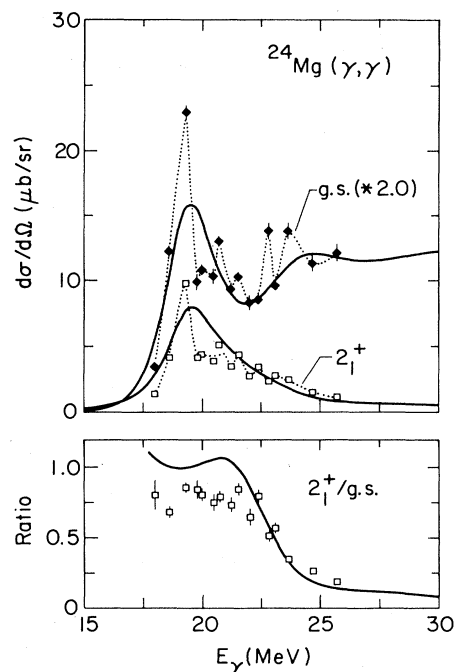


FIG. 2. Elastic and 2_1^+ inelastic cross sections at 135° on ^{24}Mg . Also shown is the ratio of inelastic to elastic scattering. The curves are calculations based on the dynamic collective model, assuming that ^{24}Mg is a prolate rotor.

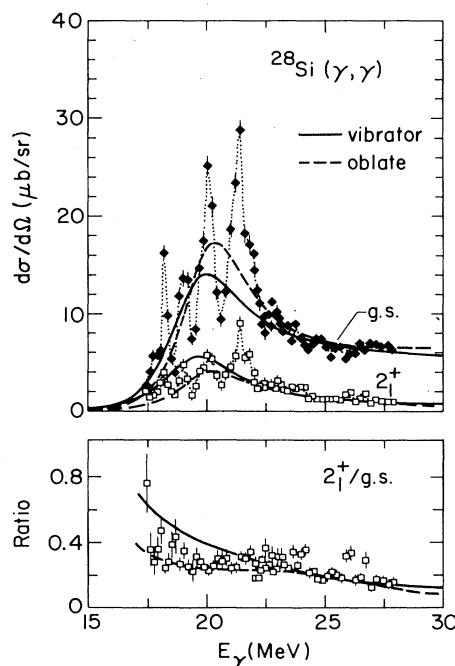


FIG. 3. Elastic and 2_1^+ inelastic cross sections at 135° on ^{28}Si . Also shown is the ratio of inelastic to elastic scattering. The curves are calculations based on the dynamic collective model. The solid curves assume that ^{28}Si is a spherical vibrator while the dashed curves assume that ^{28}Si is an oblate rotor.

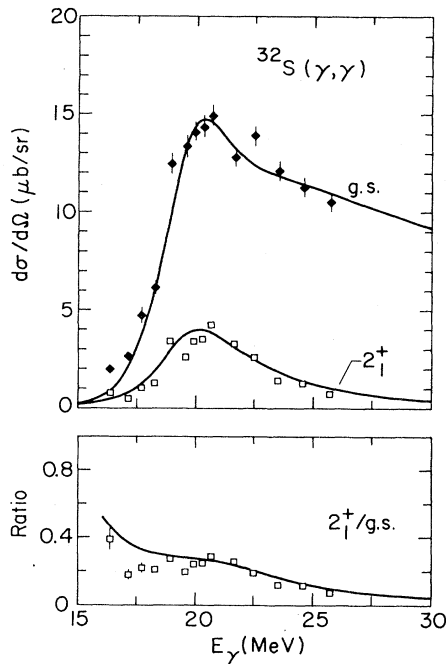


FIG. 4. Elastic and 2_1^+ inelastic cross sections at 135° on ^{32}S . Also shown is the ratio of inelastic to elastic scattering. The curves are calculations based on the dynamic collective model, assuming that ^{32}S is a spherical vibrator.

III. ANALYSIS AND DISCUSSION

A. Inelastic cross sections

The measured cross sections for elastic and inelastic photon scattering on ^{24}Mg , ^{28}Si , and ^{32}S are shown in Figs. 2, 3, and 4, respectively. Also shown are the ratio of the 2_1^+ to the elastic cross section for each nucleus. In each case we observe that the gross structure of the elastic data is strongly correlated with the 2_1^+ data; i.e., the branching ratio remains relatively constant throughout the GDR region. The branching ratios are approximately 30% for ^{28}Si and ^{32}S and around 80% for ^{24}Mg . For ^{24}Mg and ^{28}Si , these results are qualitatively quite different from the structure seen in the $^{27}\text{Al}(p,\gamma)^{28}\text{Si}$ or $^{23}\text{Na}(p,\gamma)^{24}\text{Mg}$ reactions. In these latter reactions the γ_0 and γ_1 excitation functions look essentially identical, except that the γ_1 excitation function is shifted upwards in energy relative to the γ_0 excitation function by the excitation energy of the first excited state. This is exactly in line with the picture of Brink¹⁴ and Axel¹⁵ in which each level of the nucleus has built upon it a GDR, shifted upwards in energy by the excitation energy of that level. Whereas the (p,γ) reaction maps out the giant resonances built on the ground and excited states,¹⁶ the present inelastic scattering data probe the coupling between the giant resonances built on the ground and 2_1^+ states.

Although fully microscopic shell-model calculations of the photon decay branches of the GDR for these nuclei do not exist, the trend is that the branching ratio to the

2_1^+ state is small for those nuclei with closed subshells in the ground state, while the branching ratio is large for those nuclei with an open subshell. This can be qualitatively understood as follows.¹⁷ For ^{24}Mg , the shell-model wave function for the 2_1^+ state has for its largest component the $(d_{5/2})^8$ configuration¹⁸ which is mainly a rearrangement of nucleons in the open subshell. Thus the possibility exists for a large overlap between the GDR built on the ground state and the 2_1^+ state. On the other hand, the shell-model wave function of the 2_1^+ state of ^{28}Si is dominated by the one-hole-one-particle $(d_{5/2})^{11}-(s_{1/2})^1$ configuration¹⁸ and therefore the GDR built on that level is predominantly a 2p-2h excitation relative to the closed subshell. Thus one expects little overlap with the ground-state GDR. A similar agreement holds for ^{32}S where the shell-model wave function of the 2_1^+ state has for its leading components the $(d_{5/2})^{12}-(s_{1/2})^3-(d_{3/2})^1$ (21%) and $(d_{5/2})^{12}-(s_{1/2})^1-(d_{3/2})^3$ (15%) configurations.¹⁸

An alternate way to look at the data is in the context of the dynamic collective model.^{10,19} The DCM is an extension of the hydrodynamic model in which the nucleus is treated as a liquid drop with a well-defined surface and a constant density in the interior. The nucleus possesses two types of collective degrees of freedom, namely vibrations of the nuclear surface and density fluctuations of the neutron and proton fluids. The coupling between these different collective degrees of freedom arises because the frequency of the dipole mode is proportional to the inverse of the nuclear radius. Therefore the high frequency dipole vibrations are modulated by the lower frequency surface vibrations, leading to an almost classical problem in the coupling of normal modes. Qualitatively, for nuclei that are "soft" vibrators (i.e., low frequency, large amplitude) one expects a strong coupling between the dipole and surface modes, leading to a fractionation of the dipole strength into vibrational satellite peaks and a substantial photon decay branch of the GDR to low-lying vibrational levels. The opposite is expected for "stiff" vibrators (i.e., high frequency, small amplitude). Thus the photon decay branches in vibrational nuclei probe the coupling between the dipole and surface modes.¹⁹ On the other hand, for statically deformed, axially symmetric nuclei, the GDR built on the ground and 2_1^+ rotational levels completely mix, resulting in a splitting of the GDR into $K=0$ and $K=1$ modes, corresponding to dipole oscillations along and normal to the symmetry axis, respectively. The energy splitting of the two modes is directly related to the intrinsic deformation: for prolate nuclei the $K=0$ mode lies lower while for oblate nuclei the $K=1$ mode lies lower.²⁰ Straightforward angular momentum coupling rules allow one to uniquely calculate the ratio

$$R = \frac{B(E1; 1^-, K \rightarrow 0_1^+)}{B(E1; 1^-, K \rightarrow 2_1^+)}$$

This ratio is 0.5 for the $K=0$ mode and 2.0 for the $K=1$ mode.²¹ Thus the photon decay branches in deformed nuclei probe the K quantum number of the dipole mode.

The DCM has met with considerable success when applied to medium and heavy nuclei.^{7,9,8} For light nuclei one no longer expects the hydrodynamic model or the DCM to provide a detailed description of the GDR. Nevertheless, the collective nature of the 2_1^+ states of ^{24}Mg , ^{28}Si , and ^{32}S is supported by the fact that the reduced transition probability $B(E2; 2_1^+ \rightarrow \text{g.s.})$ is several single-particle units for all these nuclei.¹³ As a consequence sizable nuclear deformations and/or vibrational amplitudes are suggested. Thus we have decided to examine the coupling of the GDR to the surface degrees of freedom for the present sd -shell nuclei in the framework of the DCM. For ^{32}S , the 2_1^+ level was treated as a vibration whose frequency and amplitude are completely determined in the harmonic approximation by the energy $E_{2_1^+}$ and the transition strength $B(E2; 2_1^+ \rightarrow \text{g.s.})$. For ^{24}Mg , the 2_1^+ level was treated as the 2^+ member of the ground-state rotational band. The deformation, assumed prolate, is determined from $B(E2; 2_1^+ \rightarrow \text{g.s.})$. For ^{28}Si , two different calculations were performed: one in which the 2_1^+ level was treated as a vibration and another in which it was treated as the 2_1^+ member of the ground-state rotational band in an oblate-deformed nucleus.

The DCM calculations were performed using the computer code CNM.⁸ Briefly, the code calculates the energies of the various vibrational and/or rotational components of the GDR as well as the dipole matrix elements connecting these states to the ground and 2_1^+ states. Each dipole state is treated as a Lorentzian resonance whose damping width is not prescribed by the model. For the present calculations, we assumed a power-law energy dependence to the widths and adjusted the parameters to best fit the elastic scattering data. Once the energies, matrix elements, and widths are specified, the photon scattering cross sections can be calculated and compared to the data. The relevant formulas are given in the literature.⁷

The comparisons are made in Figs. 2–4. It is immediately clear that the DCM can only account for the average behavior of the cross sections and in particular cannot reproduce the rapid fluctuations in ^{28}Si . These fluctuations have a different origin and will be discussed in the next section. However, the DCM does a remarkable job at predicting the average energy dependence of the cross sections as well as the overall magnitude of the ratio of inelastic to elastic scattering. In particular it is able to account for the similarities between ^{32}S and ^{28}Si and the differences between these and ^{24}Mg . The relatively small ratio for ^{32}S arises since the coupling is due to the vibrational nature of the 2_1^+ level. Both the magnitude (20–30 %) and energy dependence of this ratio is quite typical of ratios observed in medium and heavy vibrational nuclei.⁷ On the other hand, the much larger ratio in ^{24}Mg is exactly what is expected and observed in strongly deformed prolate nuclei.^{9,8} In both these cases, the DCM calculation is able to account for the behavior of this ratio. For ^{28}Si the data are equally well described by both the vibrational and the oblate-deformed hypothesis: the scattering data cannot distinguish these two possibilities. However, there is considerable experimental and theoret-

ical evidence that ^{28}Si is oblate. The principal experimental evidence comes from the sign of the quadrupole moment $Q_{2_1^+}$, which is positive (indicating oblate) for ^{28}Si and negative (indicating prolate) for ^{24}Mg .¹³ The signs and magnitudes of $Q_{2_1^+}$ for these nuclei are also predicted by recent shell-model calculations,¹⁸ and they agree well with the data. In the language of the collective model, both the experimental evidence and the shell-model calculations indicate a strong prolate deformation for the lower part of the sd shell, extending at least through ^{24}Mg and an unambiguously sharp transition to oblate deformation at ^{28}Si . The photon scattering data are completely consistent with that description, at least in the framework of the DCM: more inelastic scattering is expected and observed in the prolate ^{24}Mg than in the oblate ^{28}Si . For ^{32}S , both the experimental and calculated $Q_{2_1^+}$ are negative, indicating either a prolate deformation or an anharmonic vibrator. The inelastic scattering data show a clear preference for the vibrational hypothesis. It is interesting to point out the sensitivity of photon scattering to distinguish between prolate and oblate deformations and between rotational and vibrational nuclei. Data for the 2_1^+ level seem to be sufficient to make the distinction, while other reactions involving the inelastic scattering of hadrons require scattering data for several excited states in order to make meaningful distinctions.²² We further note that the present data for ^{32}S indicate that the role played by anharmonicities in describing the elastic and 2_1^+ -inelastic scattering is rather small, in good agreement with results obtained using light hadronic probes.²²

B. Cross section fluctuations in ^{28}Si

The remarkable feature of the GDR of ^{28}Si is the fractionation of the resonance into four relatively narrow peaks between 18 and 22 MeV. Equally remarkable is that this structure is reflected in both the elastic and the inelastic cross sections and that despite the fluctuating nature of these cross sections, the *ratio* of inelastic to elastic scattering varies smoothly with energy. These fluctuations are not unique to the photon scattering experiment and have been observed in other photonuclear reactions such as total photoabsorption,²³ total photoproton,²⁴ total photoneutron,²⁵ and $^{27}\text{Al}(p, \gamma_0)^{28}\text{Si}$.²⁶ Indeed, the fluctuations seen in photon scattering track quite well with the fluctuations seen in other experiments.

In this section we address these fluctuations in terms of the implications for the total photoabsorption cross section σ_γ . To this end we utilize the unique relationship between σ_γ and the elastic scattering cross section $d\sigma/d\Omega$. One can *exactly* and *uniquely* predict $d\sigma/d\Omega$ from σ_γ using the optical theorem, a dispersion relation, the dipole angular distribution, and the Thomson amplitude (corrected for finite nuclear size and exchange effects). The formalism has been thoroughly discussed in the literature.¹² A comparison is made in Fig. 5. The points are the present elastic cross sections and the dotted curve is the predicted cross section based on the ex-

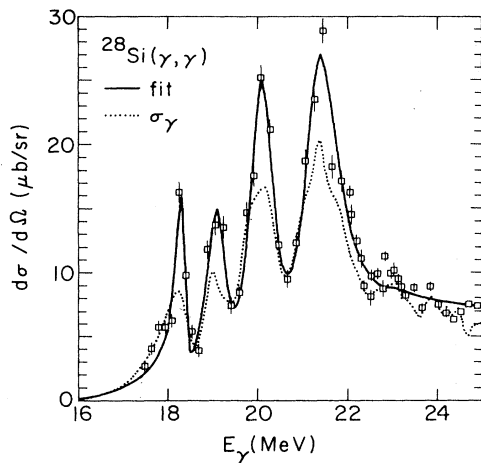


FIG. 5. Elastic scattering cross sections at 135° on ^{28}Si . The dotted curve is the predicted cross section based on the Mainz measurements of the total photoabsorption cross section. The solid curve is the predicted cross section based on a multi-Lorentzian parametrization of the total photoabsorption cross section, with parameters adjusted to fit the scattering data.

perimental values of σ_γ measured at Mainz.²³ This latter cross section is shown as the points in Fig. 6. The predicted elastic scattering cross section has been averaged over the 160-keV resolution of the present experiment. We emphasize that we have not done a fit to the scattering data but rather a calculation based on absolute cross sections, with no arbitrary normalization. We see in Fig. 5 that above 22.5 MeV, where both σ_γ and $d\sigma/d\Omega$ vary smoothly with energy, the dotted curve agrees well with the data. This curve also agrees with the data at the minimum of the structures in the cross section below 22.5 MeV. However, the curve falls below the peak of the structures in the 18–22-MeV region. This does not necessarily mean that the two sets of cross sections

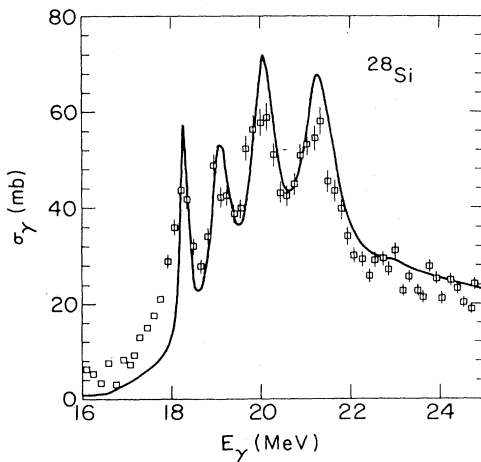


FIG. 6. The Mainz measurements of the total photoabsorption cross section. The curve is the multi-Lorentzian parametrization of this cross section that best fits the elastic scattering data (Fig. 5).

($d\sigma/d\Omega$ and σ_γ) are incompatible. One should realize that the σ_γ data in Fig. 6 represent averages over a 0.2–0.3-MeV energy interval. Since elastic scattering involves both the absorption and the emission of a dipole photon, $d\sigma/d\Omega$ should scale roughly with the square of σ_γ . Since the average of the square of a fluctuating quantity is larger than the square of the average of that quantity, the procedure used to derive the dotted curve in Fig. 5 will *underpredict* the scattering cross section if there is unresolved fine structure in σ_γ . Therefore the relation between the calculation and the data in Fig. 5 is exactly what one would expect if the peaks in σ_γ are actually narrower than implied by the data of Fig. 6 and/or if those peaks actually represent an energy average of even finer structure. It is not possible to distinguish these two possibilities with the present scattering data, although there is supporting evidence for both possibilities from other reactions.

There is strong evidence from the total photoproton reaction²⁴ that the intermediate structure bumps are narrower than implied by the Mainz σ_γ . The photoproton data have incident photon resolution comparable to the photon scattering experiment, and when these data are added to the total photoneutron data, the structures in the resulting sum are both taller and narrower than the corresponding structures in the Mainz σ_γ . The present scattering data are consistent with this result. In order to demonstrate this point, we parametrize σ_γ as a sum of several Lorentzian lines and use this parametrization to predict $d\sigma/d\Omega$. We then adjust the parameters of each Lorentzian (peak cross section, centroid, and width) in order to best fit the elastic scattering data. In that way, we determine a σ_γ that is consistent with the elastic data. The resulting fit is shown as the solid curve in Fig. 5, and the corresponding σ_γ is compared to the Mainz data in Fig. 6. We see that indeed the structures in this inferred σ_γ are both taller and narrower than the corresponding structures in the Mainz data.

There is also supporting evidence in the literature for unresolved fine structure, principally from the $^{27}\text{Al}(p, \gamma_0)^{28}\text{Si}$ reaction.²⁶ These data, which have an energy resolution of 15 keV, show a severe splitting of the four main peaks of the GDR into much narrower peaks with an average spacing of about 120 keV. The near constancy of the interval between each peak across the entire GDR region suggests that the observed structure is not due to individual levels of the excited system. This suggestion is supported by estimates that the expected spacing between levels is much smaller (10–15 keV) and that the levels are moderately to strongly overlapping. It was suggested that the fine structure is instead due to so-called “Ericson fluctuations,”²⁷ which result from the random nature of the interfering amplitudes among many overlapping levels. Normally one does not expect Ericson fluctuations to persist in the total cross section, σ_γ , since the contributions of the various decay channels would be expected to effectively average out the fluctuations. In the case of the GDR in ^{28}Si , the p_0 decay channel is prominent enough that it is possible that the fluctuations could persist in the total cross section. Of

course, one could easily decide this issue if one could measure either σ_γ or $d\sigma/d\Omega$ with better than about 30-keV resolution. Alternately, one can use poorer resolution scattering data, like the present results, to see if they are at least consistent with fine structure in σ_γ . We demonstrate this in Fig. 7. The points are the present elastic scattering data and the curves are predicted cross sections, averaged over 160 keV, based on the (γ, p_0) cross section, which was obtained by detailed balance from the $^{27}\text{Al}(p, \gamma_0)^{28}\text{Si}$ data.²⁶ In the solid curve, the optical theorem and dispersion relation are applied directly to the (γ, p_0) data, and the result is then scaled to best fit the scattering data. In the dotted curve, a similar procedure is used except that the (γ, p_0) data are first averaged over 200 keV before applying the optical theorem and dispersion relation. The difference between the two curves represents the effect of unresolved fine structure on the elastic scattering cross section. As discussed qualitatively above, the main effect is to enhance the elastic cross section over that expected for a smooth photoabsorption cross section. Without attempting to be more quantitative than this, it is clear that such an effect could account for the discrepancy between the scattering data and the Mainz σ_γ .

We have already noted that despite the structure in σ_γ , the ratio of inelastic to elastic photon scattering varies smoothly throughout the GDR region. It was originally hoped that the observation of variations in the photon decay branch to the 2_1^+ level might help elucidate the nature of the four peaks in σ_γ . For example, it might have allowed us to assign a K quantum number to each peak, as discussed above. However, the constancy of this branching ratio has taught us nothing in detail; instead it

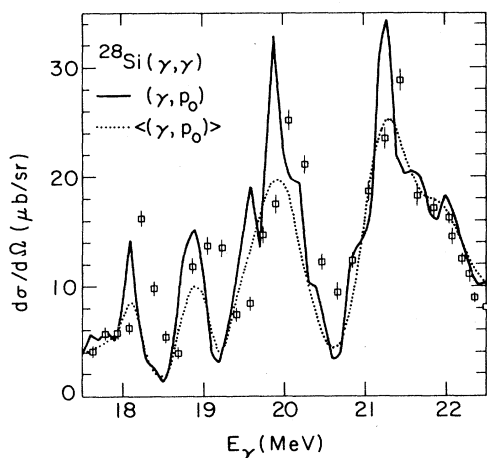


FIG. 7. A demonstration of the effect of unresolved fine structure on the elastic scattering cross section. The curves were calculated using the high resolution (γ, p_0) data to predict the elastic scattering cross section, averaged over 160 keV. The solid curve uses the (γ, p_0) data directly, whereas the dotted curve first averages the (γ, p_0) data over 200 keV. The points are the present elastic scattering cross sections on ^{28}Si .

suggests that the mechanism responsible for the mixing of the GDR's built on the ground and the 2_1^+ states is quite different from the mechanism responsible for the fractionation of the GDR into four peaks. For example, in the DCM one starts with a single dipole level built on the ground state, which then mixes with the GDR built on the 2_1^+ state. This mechanism alone would give rise to inelastic-to-elastic ratios that vary smoothly with energy, as seen in Fig. 3. Whatever mechanism is responsible for the further fractionation of the dipole strength affects the elastic and inelastic cross sections in exactly the same way, thereby maintaining the smooth energy dependence of the cross section ratios. Apparently the fractionation involves the coupling to more complicated, possibly non-collective degrees of freedom.

The idea of a single, highly collective GDR "doorway" state that couples to more complicated degrees of freedom is not a new one. For example, it was long ago observed²⁶ that the angular distribution of photons from $^{27}\text{Al}(p, \gamma)^{28}\text{Si}$ reaction is relatively constant across the entire GDR. More recent data on $^{28}\text{Si}(e, e'x)$ seem to indicate that the transition charge density of the GDR does not vary across all the structure in the cross section.²⁸ The present data provide additional confirming evidence. To our knowledge, there is as yet no adequate theoretical explanation for the fractionation of dipole strength in the GDR of ^{28}Si .

IV. SUMMARY AND CONCLUSIONS

We have measured cross sections for the elastic and inelastic scattering of monochromatic photons in the GDR region of ^{24}Mg , ^{28}Si , and ^{32}S . We have analyzed these data in terms of the coupling between the GDR's built on the ground and 2_1^+ states. Qualitatively, we find that for those nuclei with mainly closed subshell configurations in the ground state (i.e., ^{28}Si and ^{32}S), the inelastic-to-elastic scattering ratio is small, while for those nuclei with mainly open subshell configurations in the ground state (i.e., ^{24}Mg), this ratio is large. This trend can be roughly explained with a simple shell-model picture. Somewhat more quantitatively, we find excellent agreement between the energy-averaged cross sections and the predictions of the dynamic collective model. When interpreted in terms of this model, the data confirm other experimental evidence that ^{32}S is a spherical vibrator while ^{24}Mg and ^{28}Si are prolate and oblate rotors, respectively.

For ^{28}Si there is considerable structure in the scattering cross sections that is not predicted by the DCM. We have used the elastic scattering data to infer the total photoabsorption cross section. We conclude that this inferred cross section is somewhat more structured than previous direct measurements of the photoabsorption. Despite this structure, the inelastic-to-elastic ratios vary only smoothly with energy, suggesting that the mechanism for the fractionation of the GDR into four peaks has a very different origin from the mechanism responsible for the coupling between the GDR's built on the ground and 2_1^+ states.

ACKNOWLEDGMENTS

We acknowledge several interesting and fruitful discussions concerning the shell-model interpretation of the

data with Dr. B. A. Brown. This research was supported by the National Science Foundation under Grant No. NSF PHY 86-10493.

- ¹R. A. Eramzhyan, B. S. Ishkhanov, I. M. Kapitonov, and V. G. Neudatchin, Phys. Rep. **136**, 229 (1986).
- ²S. A. Farris and J. M. Eisenberg, Nucl. Phys. **88**, 241 (1966).
- ³D. Drechsel, J. B. Seaborn, and W. Greiner, Phys. Rev. **162**, 983 (1967).
- ⁴W. H. Bassichis and F. Scheck, Phys. Rev. **145**, 771 (1966).
- ⁵S. S. M. Wong, D. J. Rowe, and J. C. Parikh, Phys. Lett. **48B**, 403 (1974).
- ⁶K. A. Snover, Annu. Rev. Nucl. Part. Sci. **36**, 1 (1986).
- ⁷T. J. Bowles, R. J. Holt, H. E. Jackson, R. M. Laszewski, R. D. McKeown, A. M. Nathan, and J. R. Specht, Phys. Rev. C **24**, 1940 (1981).
- ⁸S. D. Hoblit, Ph.D. thesis, University of Illinois, 1988; S. D. Hoblit and A. M. Nathan (unpublished).
- ⁹A. M. Nathan and R. Moreh, Phys. Lett. **91B**, 38 (1980); A. M. Nathan, Phys. Rev. C **38**, 92 (1988).
- ¹⁰M. Danos and W. Greiner, Phys. Rev. **134**, B284 (1964).
- ¹¹J. J. Sakurai, *Advanced Quantum Mechanics* (Addison-Wesley, Reading, MA, 1975), p. 57ff.
- ¹²D. H. Wright, P. T. Debevec, L. J. Morford, and A. M. Nathan, Phys. Rev. C **32**, 1174 (1985).
- ¹³P. M. Endt, At. Data Nucl. Data Tables **23**, 3 (1979).
- ¹⁴D. M. Brink, D. Phil. thesis, University of Oxford, 1955.
- ¹⁵P. Axel, Phys. Rev. **126**, 671 (1962).
- ¹⁶D. H. Dowell, G. Feldman, K. A. Snover, A. M. Sandorfi, and M. T. Collins, Phys. Rev. Lett. **50**, 1191 (1983).
- ¹⁷B. A. Brown, private communication.
- ¹⁸M. Cardichi, B. H. Wildenthal, and B. A. Brown, Phys. Rev. C **34**, 2280 (1986).
- ¹⁹J. Eisenberg and W. Greiner, *Nuclear Models* (North-Holland, Amsterdam, 1970), p. 331ff.
- ²⁰M. Danos, Nucl. Phys. **5**, 23 (1958); K. Okamoto, Phys. Rev. **110**, 143 (1958).
- ²¹A. Bohr and B. Mottleson, *Nuclear Structure* (Benjamin, Reading, MA, 1975), Vol. II, p. 453ff.
- ²²R. Alarcon and J. Rapaport, Nucl. Phys. **A458**, 502 (1986); G. Haouat *et al.*, Phys. Rev. C **30**, 1795 (1984).
- ²³J. Ahrens, H. Borchert, K. H. Czoek, H. B. Eppler, H. Gimm, H. Gundrum, M. Kroning, P. Riehn, G. Sita Ram, A. Zieger, and B. Ziegler, Nucl. Phys. **A251**, 479 (1975).
- ²⁴R. L. Gulbranson, L. S. Cardman, A. Doron, A. Erell, K. R. Lindgren, and A. I. Yavin, Phys. Rev. C **27**, 470 (1983).
- ²⁵A. Veyssière, H. Beil, R. Bergère, P. Carlos, A. Leprêtre, and A. de Miniac, Nucl. Phys. **A227**, 513 (1974).
- ²⁶P. P. Singh, R. E. Segel, L. Meyer-Schützmeister, S. S. Hanna, and R. G. Allas, Nucl. Phys. **65**, 577 (1965).
- ²⁷T. E. O. Ericson, Ann. Phys. (N.Y.) **23**, 390 (1963).
- ²⁸Th. Kihm, K. T. Knöpfle, H. Riedesel, P. Voruganti, H. J. Emrich, G. Fricke, R. Neuhausen, and R. K. M. Schneider, Phys. Rev. Lett. **56**, 2789 (1986).